

Shape Outlier Detection and Visualization for Functional Data: the Outliergram

Ana Arribas-Gil* and Juan Romo

Departamento de Estadística

Universidad Carlos III de Madrid, Getafe, Spain.

E-mail: ana.arribas@uc3m.es, juan.romo@uc3m.es

September 9, 2018

Abstract

We propose a new method to visualize and detect shape outliers in samples of curves. In functional data analysis we observe curves defined over a given real interval and shape outliers are those curves that exhibit a different shape from the rest of the sample. Whereas magnitude outliers, that is, curves that exhibit atypically high or low values at some points or across the whole interval, are in general easy to identify, shape outliers are often masked among the rest of the curves and thus difficult to detect. In this article we exploit the relation between two depths for functional data to help visualizing curves in terms of shape and to develop an algorithm for shape outlier detection. We illustrate the use of the visualization tool, the outliergram, through several examples and asses the performance of the algorithm on a simulation study. We apply them to the detection of outliers in a

*Corresponding author

children growth dataset in which the girls sample is contaminated with boys curves and viceversa.

Keywords: Depth for functional data; Outlier visualization; Robust estimation.

1 Introduction

In many every day life applications, individual observations are real functions of time, observed at discrete time points. Each curve provides the evolution over time of a certain process of interest for a given individual. When the grid of points is dense enough, and the underlying process is known to be continuous, curves can be treated as functional data. In this context, data can be seen as a sample of curves, in which it is common to observe outlying trajectories. Examples include human growth curves, time-course microarray experiments, daily curves of electricity consumption or annual curves of daily mean temperature among others.

As in the univariate or the multivariate case, the presence of atypical observations may affect the statistical analysis of the data. Then, any preliminary analysis should include an outlier detection step. The challenge in the functional framework is that outlying observations might be very difficult to identify visually. Indeed, an outlier trajectory is not only one that contains atypically high or low values but also a trajectory that even containing average levels across the whole observation interval may present a different shape or pattern than the rest of the curves of the sample. We will refer to the first type of atypical curves as magnitude outliers and to the second one as shape outliers. Whereas magnitude outliers might be easily detected even with a simple visual inspection of the data, shape outliers will be *hidden* in the middle of the sample and its identification will not be straightforward. That is, a shape outlier is not an observation that lies far away from the sample in terms of the Euclidean distance. Then,

measures that can deal with shape features need to be considered in order to be able to distinguish them from the rest of the curves. In this article we combine two sources of information about curve shape given by two measures of depth for functional data, the modified band depth (López-Pintado and Romo 2009) and the modified epigraph index (López-Pintado and Romo 2011). Each one provides an ordering of the sample according to different shape features and the relation between them sheds light on shape variation across the sample.

Different methods for outlier detection in functional data have been developed during the last years. Among them several rely on different notions of functional depth (Febrero et al. 2008; Sun and Genton 2011; Gervini 2012; Martín-Barragán et al. 2012), on robust principal components (Hyndman and Shang 2010) or on random projections of infinite dimensional data into \mathbb{R} (Fraiman and Svarc 2013). Also, some distributional approaches have been considered (Gervini 2009). While some of these methods may only be sensitive to magnitude outliers, most of them work efficiently at detecting different kinds of outlying trajectories. However, the mechanisms they rely on do not always allow to provide an easy interpretation on why an observation is considered an outlier. In this sense the objective of this article is two-fold. On the one hand, we propose an algorithm for shape outlier detection. On the other hand, we give a visualization tool that helps understanding shape variation across the sample and provides additional information that can be used to correct the output of the algorithm.

The rest of the article is as follows. In Section 2 we review the definitions of modified band depth and modified epigraph index and investigate their relationship on a sample of curves. Based on it, in Section 3 we propose a visualization tool that helps identifying curves with different shape and propose a rule for shape outliers detection. We compare our method to previous existing techniques for outlier detection in functional data through an extensive simulation study in Section 4. In Section 5 we apply our method to the

Berkeley growth dataset in which we contaminate male and female samples with height curves from the opposite sex and show its performance on detecting such outliers in comparison with other methods. Finally, we conclude the article with a discussion on Section 6.

2 Modified Band Depth and Modified Epigraph Index

Let us introduce the modified band depth (MBD) and modified epigraph index (MEI), as firstly defined in López-Pintado and Romo (2009) and López-Pintado and Romo (2011), respectively. Both measures provide an idea of how central or deep a curve is with respect to a sample of curves. Let x_1, \dots, x_n be n continuous functions defined on a given closed real interval \mathcal{I} . For any $x \in \{x_1, \dots, x_n\}$ we define its modified band depth as:

$$MBD_{\{x_1, \dots, x_n\}}(x) = \binom{n}{2}^{-1} \sum_{i=1}^n \sum_{j=i+1}^n \frac{\lambda(\{t \in \mathcal{I}, \min(x_i(t), x_j(t)) \leq x(t) \leq \max(x_i(t), x_j(t))\})}{\lambda(\mathcal{I})}$$

where $\lambda(\cdot)$ stands for the Lebesgue measure on \mathbb{R} . If for each pair of curves, x_i and x_j , in the sample we consider the band that they define in $\mathcal{I} \times \mathbb{R}$ as $\{(t, y), t \in \mathcal{I}, \min(x_i(t), x_j(t)) \leq y \leq \max(x_i(t), x_j(t))\}$, then $MBD_{\{x_1, \dots, x_n\}}(x)$ represents the mean over all possible bands of the proportion of time that $x(t)$ spends inside a band. The modified band depth is an extension of the original band depth that accounts for the proportion of bands in which a curve is entirely contained (see López-Pintado and Romo (2009) for details).

The modified epigraph index of $x \in \{x_1, \dots, x_n\}$ is defined as:

$$MEI_{\{x_1, \dots, x_n\}}(x) = \frac{1}{n} \sum_{i=1}^n \frac{\lambda(\{t \in \mathcal{I}, x_i(t) \geq x(t)\})}{\lambda(\mathcal{I})}$$

and it stands for the mean proportion of time that x lies below the curves of the sample.

As in the case of the MBD, the MEI is a generalization of the epigraph index that accounts for the proportion of curves that lie entirely above x (López-Pintado and Romo 2011).

It is clear that MBD and MEI are closely related quantities and that investigating the relation between these two measures might shed light on shape characterization of curves. Indeed, consider a curve with a modified epigraph index close to 0.5. That would mean that the curve is located in the center of the sample in terms of level variation. Then, if the curve's shape is similar to the shapes of the rest of the curves in the sample, one may expect to get a high value for its MBD, since the curve should be contained in many bands defined by other curves. However, if one gets a low MBD value, that would indicate that the curve is contained in a small number of bands, even if it is placed in the center of the sample in terms of level. That can only mean that the curve exhibits a shape very different from those of the rest of the curves.

In this section we want to investigate the relation between these two measures in order to characterize shape outlyingness. The following equality gives an expression of MBD in terms of MEI. The proof is given in the Appendix.

Remark 1. *Let x_1, \dots, x_n be n continuous functions on \mathcal{I} . Then, for any $x \in \{x_1, \dots, x_n\}$*

$$MBD_{\{x_1, \dots, x_n\}}(x) = a_0 + a_1 MEI_{\{x_1, \dots, x_n\}}(x) + a_2 \left[\sum_{i=1}^n \sum_{j=1}^n \frac{\lambda(E_{i,x} \cap E_{j,x})}{\lambda(\mathcal{I})} \right]$$

with $a_0 = a_2 = \frac{-2}{n(n-1)}$, $a_1 = \frac{2(n+1)}{n-1}$ and $E_{i,x} = \{t \in \mathcal{I}, x_i(t) \geq x(t)\}$.

Remark 2. *From Remark 1 we get*

$$MBD_{\{x_1, \dots, x_n\}}(x) = a_0 + a_1 MEI_{\{x_1, \dots, x_n\}}(x) + a_2 n^2 MEI_{\{x_1, \dots, x_n\}}(x)^2 + a_2 \left[\sum_{i=1}^n \sum_{j=1}^n \left(\frac{\lambda(E_{i,x} \cap E_{j,x})}{\lambda(\mathcal{I})} - \frac{\lambda(E_{i,x})\lambda(E_{j,x})}{\lambda(\mathcal{I})^2} \right) \right].$$

Remark 3. For any sample x_1, \dots, x_n of continuous functions on \mathcal{I} , it holds that for any $x \in \{x_1, \dots, x_n\}$,

$$MBD_{\{x_1, \dots, x_n\}}(x) \leq a_0 + a_1 MEI_{\{x_1, \dots, x_n\}}(x) + a_2 n^2 MEI_{\{x_1, \dots, x_n\}}(x)^2. \quad (1)$$

Indeed,

$$\sum_{i=1}^n \sum_{j=1}^n \left(\frac{\lambda(E_{i,x} \cap E_{j,x})}{\lambda(\mathcal{I})} - \frac{\lambda(E_{i,x})\lambda(E_{j,x})}{\lambda(\mathcal{I})^2} \right) = \int_{\mathcal{I}} a_x(t)^2 \frac{1}{\lambda(\mathcal{I})} dt - \left(\int_{\mathcal{I}} a_x(t) \frac{1}{\lambda(\mathcal{I})} dt \right)^2 \geq 0$$

from Jensen's inequality, where $a_x(t)$ is the number of curves above or equal to x at time t . Then, since $a_2 < 0$ (1) holds from Remark 2.

Moreover, if none of the curves in the sample cross each other on \mathcal{I} , that is, if $(x_i(t_1) - x_j(t_1))(x_i(t_2) - x_j(t_2)) > 0 \forall t_1, t_2 \in \mathcal{I}, \forall i \neq j$, then we have for any $x \in \{x_1, \dots, x_n\}$

$$MBD_{\{x_1, \dots, x_n\}}(x) = a_0 + a_1 MEI_{\{x_1, \dots, x_n\}}(x) + a_2 n^2 MEI_{\{x_1, \dots, x_n\}}(x)^2,$$

since in that case $E_{i,x} = \emptyset$ or $E_{i,x} = \mathcal{I}$ for all i and so, $\lambda(E_{i,x} \cap E_{j,x})/\lambda(\mathcal{I})$ and $\lambda(E_{i,x})\lambda(E_{j,x})/\lambda(\mathcal{I})^2$ are equal for all i, j . Then MBD and MEI computed over the curves of the sample define a perfect parabola.

An underlying idea below the statement of Remark 3 is that if in a sample of perfectly aligned curves with common shape one introduces a curve with a different pattern, then the \mathbb{R}^2 point corresponding to the pair (MEI, MBD) for this new curve will lie far away from the parabola defined by the points corresponding to the rest of the curves. Figure 1 provides an example of this phenomenon, in which it is very easy to detect the outlying observations by looking at the MBD vs MEI representation. In general, however, trajectories of a random process will cross many times even if they all exhibit the same trend pattern. Then, the (MEI, MBD) points will not define a perfect parabola

and identifying outlying trajectories will not be straightforward. Let us consider as an illustration the height curves of 54 girls coming from the well known Berkeley growth dataset (see Ramsay and Silverman (2005), for instance). They are presented in Figure 2 together with their MBD vs MEI representation. The points corresponding to the 3rd and 32nd girls are far from the rest of the points. These two girls exhibit a different growth pattern than the rest of the girls in the sense that they were ones of the highest of the sample during childhood and early puberty, especially true for girl number 3, but they stopped growing earlier than the rest of the girls and ended up with a height in the lower quartile at 18 year old. To what extent we can consider these two trajectories as outliers is something that can be addressed by considering the problem of outlier detection in the MBD vs MEI plane as we do in the next section.

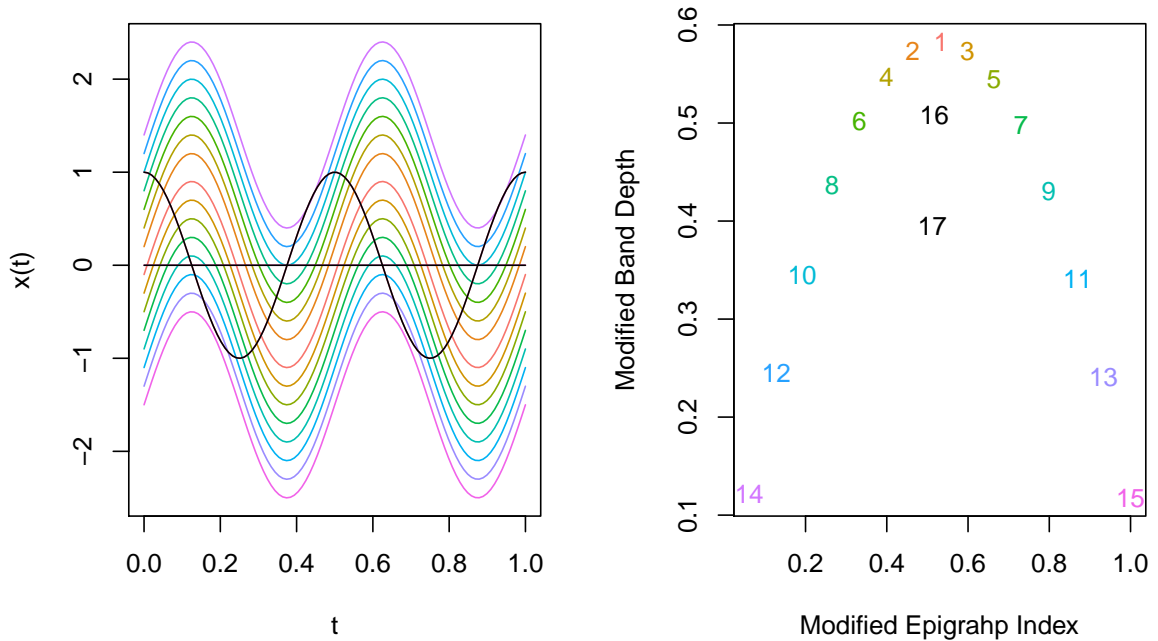


Figure 1: Left: A sample of 17 curves of the form $x_i(t) = \sin(4\pi t) + (-1)^i \frac{i}{10}$, $i = 1, \dots, 15$, $x_{16}(t) = 0$ and $x_{17}(t) = \cos(4\pi t)$, $t \in [0, 1]$. Curves x_{16} and x_{17} are displayed in black. Right: Modified band depth versus modified epigraph index of the 17 curves.

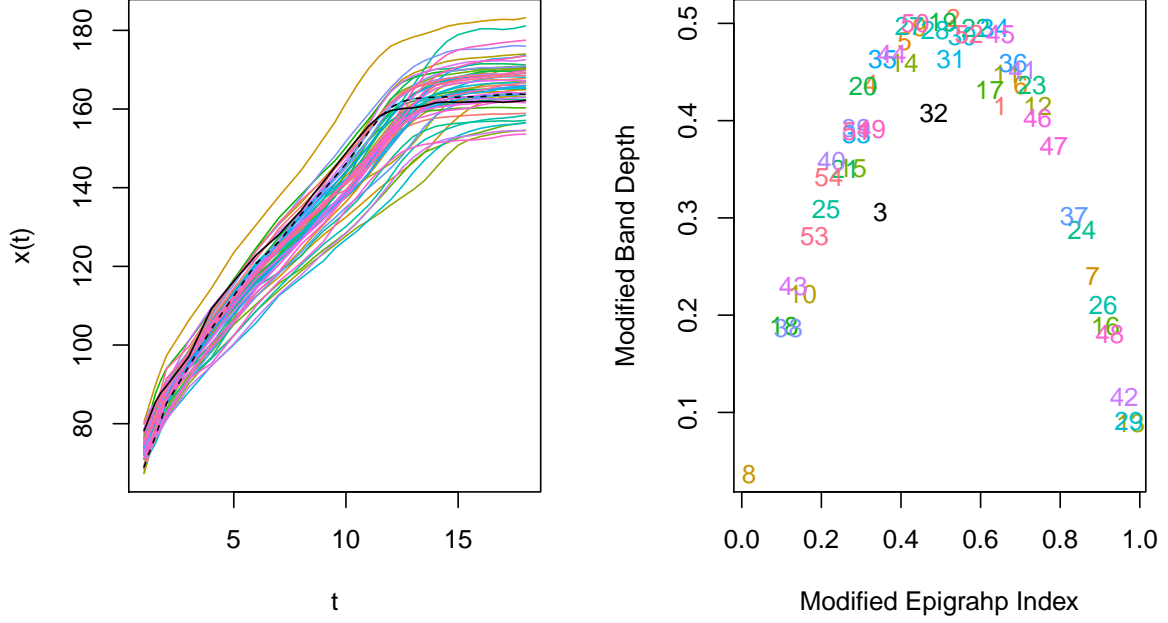


Figure 2: Left: Height curves of 54 girls during ages between 0 and 18 years. Curves x_3 and x_{32} are displayed in black with solid and dashed lines respectively. Right: Modified band depth versus modified epigraph index of the 54 curves.

3 Shape outlier detection algorithm and outliergram

Based on the relation between the modified band depth and the modified epigraph index we now propose to use the MBD vs MEI plane as a visualization tool and we give an algorithm to detect shape outliers. From Remark 3 we know that all the (MEI, MBD) points lie below the parabola given by (1) and that the closest points to the parabola correspond to curves with typical shape, whereas the most distant ones represent outlying curves in terms of shape. This motivates the use of the univariate boxplot rule for outlier detection on the vertical distances to the parabola. That is, given a sample of curves x_1, \dots, x_n with $mb_i = MBD_{x_1, \dots, x_n}(x_i)$ and $me_i = MEI_{x_1, \dots, x_n}(x_i)$ for $i = 1, \dots, n$, we consider the distances $d_i = a_0 + a_1 me_i + n^2 a_2 me_i^2 - mb_i$ and define as shape outliers those curves with $d_i \geq Q_{d3} + 1.5 IQR_d$, where Q_{d3} and IQR_d are the third quartile and

inter-quartile range of d_1, \dots, d_n . In addition to the outlier detection rule, it might be interesting to assess how distant the outliers are from the rest of the sample or to identify curves that might be close to the outlier region although not inside. To jointly visualize the observations in terms of shape and the border between the outlying and non-outlying curves we propose to represent in \mathbb{R}^2 the (MEI, MBD) points together with the parabola shifted downwards by $Q_{d3} + 1.5IQR_d$. We will refer to this graphical representation as the outliergram. In Figure 3 we present an example of such a representation. Although the outliergram has not been conceived to detect magnitude outliers, notice that these will appear at the bottom corners of the plot. The gap between them and the contiguous observations (according to the order induced by MEI) might be an indicator of their outlyingness. However we do not pretend to give a specific rule to detect them, since very good mechanisms for this purpose already exist, such as the functional boxplot defined in Sun and Genton (2011) (see also Martín-Barragán et al. (2012)). Indeed, we propose to combine that algorithm with our shape outlier detection rule.

It is worth noticing that the precedent reasoning for shape outlier detection might fail with curves that lie above or below the majority of the curves in the sample, that is, with MEI values close to 0 or 1. Indeed, for such curves the modified band depth will always be low, since they are surrounded by very few curves, independently of the fact that they might present an atypical shape or not. However, if the curve presented a typical shape and we shifted it vertically towards the center of the sample its MBD in the new location should increase (as MEI increases or decreases). On the other hand, if the curve's shape was atypical, even when placed in the center of the sample, its MBD would remain low. That motivates the addition of a second step in the shape outlier detection procedure in which the more extreme curves (see below for a proper definition) are vertically shifted towards the center of the sample one by one. They would be considered shape outliers if the new (MBD, MEI) point lies in the outlying region previously determined. In that

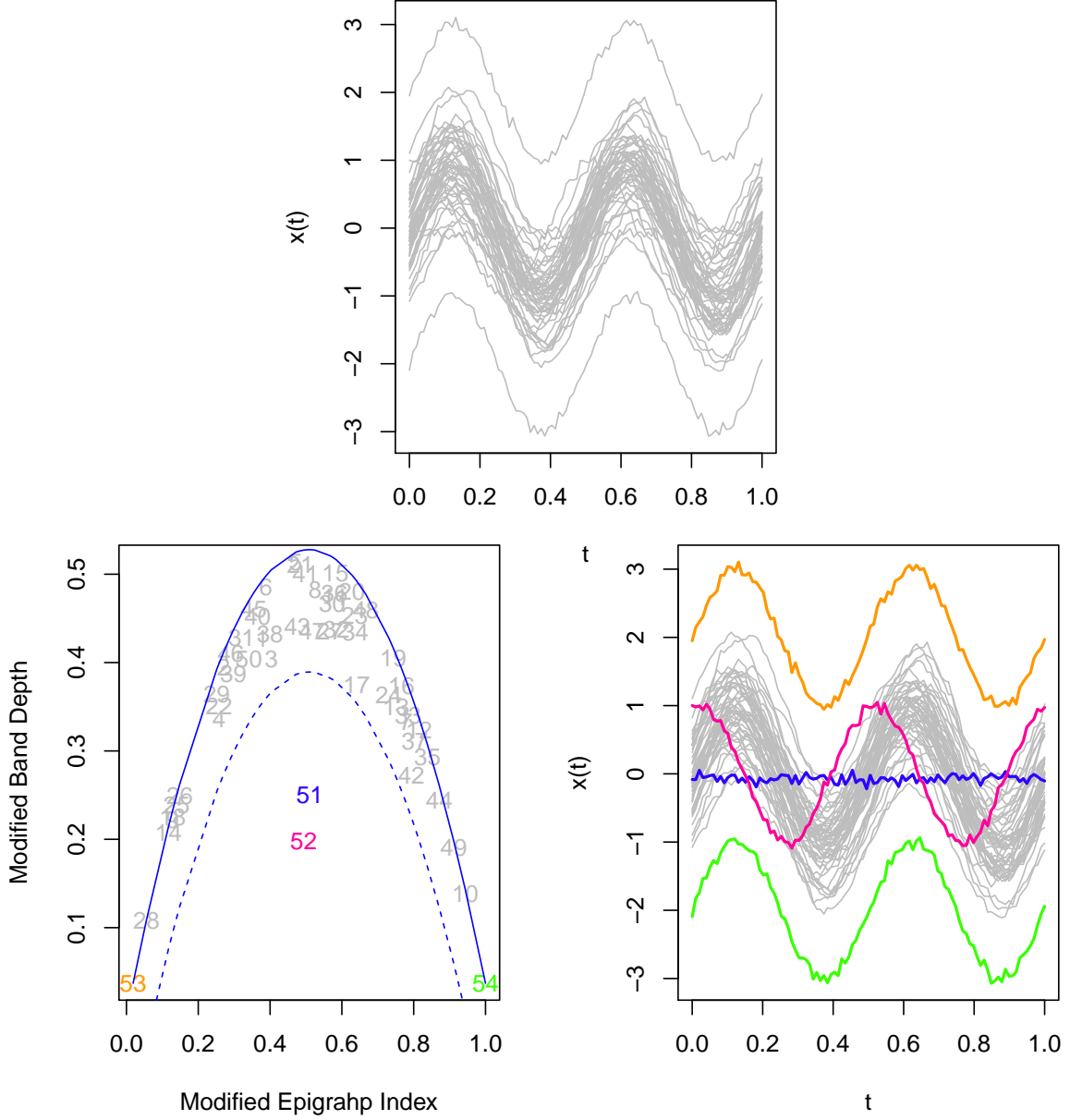


Figure 3: Top: 50 curves generated under the process $X(t) = \sin(4\pi t) + \varepsilon(t)$, $t \in [0, 1]$, where $\varepsilon(t)$ is a Gaussian process with zero mean and covariance function $\gamma(s, t) = 0.2 \exp\{-0.8|s - t|\}$, and four outliers (curves 51 to 54). Only two magnitude outliers are visually identifiable. Bottom left: Outliergram. The solid parabola is $P_i = a_0 + a_1 m e_i + n^2 a_2 m e_i^2$ and the dashed one is $P_i - Q_{d3} - 1.5 IQR$, which represents the boundary between outlying and non-outlying observations. Bottom right: same as top where magnitude outliers as well as the outliers detected by the outliergram are now shown in color. The color code is the same in both graphics.

case the outliergram will show both the old and the new (MBD,MEI) points, using a different symbol for the last one to help distinguishing them (see Figures 4 and 5 for some examples).

Then, given a sample of curves x_1, \dots, x_n , the whole outlier detection algorithm is as follows:

1. Compute $mb_i = MBD_{x_1, \dots, x_n}(x_i)$, $me_i = MEI_{x_1, \dots, x_n}(x_i)$ and $P_i = a_0 + a_1 me_i + n^2 a_2 me_i^2$, for $i = 1, \dots, n$.
2. Compute $d_i = P_i - mb_i$, for $i = 1, \dots, n$ where a_0, a_1 and a_2 are the ones given in Remark 1.
3. Compute the third quartile and inter-quartile range of the sample d_1, \dots, d_n , Q_{d3} and IQR_d .
4. Shape outlier identification: $SO = \{i \text{ s. t. } mb_i \leq P_i - Q_{d3} - 1.5IQR_d\}$.
5. For $i \in \{1, \dots, n\} \setminus SO$:
 - If $x_i(t) < \min_{j \neq i} x_j(t)$ for some $t \in \mathcal{I}$, define $\tilde{x}_i(t) = x_i(t) - \min_t \{x_i(t) - \min_{j \neq i} x_j(t)\}$.
 - If $x_i(t) > \max_{j \neq i} x_j(t)$ for some $t \in \mathcal{I}$, define $\tilde{x}_i(t) = x_i(t) - \max_t \{x_i(t) - \max_{j \neq i} x_j(t)\}$.
 - Compute $\widetilde{mb}_i = MBD_{x_1, \dots, \tilde{x}_i, \dots, x_n}(\tilde{x}_i)$, $\widetilde{me}_i = MEI_{x_1, \dots, \tilde{x}_i, \dots, x_n}(\tilde{x}_i)$ and $\widetilde{P}_i = a_0 + a_1 \widetilde{me}_i + n^2 a_2 \widetilde{me}_i^2$. If $\widetilde{mb}_i \leq \widetilde{P}_i - Q_{d3} - 1.5IQR_d$ then $SO = SO \cup \{i\}$.
6. Magnitude outlier identification: use the functional boxplot rule to identify magnitude outliers (Sun and Genton 2011).

4 Simulation study

In this section we compare the performance of the proposed procedure with several functional and/or multivariate outlier detection methods through an extensive simulation study. Namely, we consider seven different techniques developed during the last decade (the numbers below stand only for reference purposes).

1. Functional boxplot (Sun and Genton 2011): considering the center outward ordering induced by band depth or modified band depth in a sample of curves, a boxplot is constructed by defining the envelope of the 50% central region. The maximum non-outlying envelope is obtained by inflating that central region 1.5 times as in a univariate boxplot. Any curve lying partially or globally outside that maximum non-outlying envelope is considered an outlier.
2. Functional highest density region (HDR) boxplot (Hyndman and Shang 2010): a functional boxplot is obtained by construction a bivariate HDR boxplot (Hyndman 1996) to the first two robust principal component scores. The coverage probability of the outlying region needs to be prespecified.
3. Robust Mahalanobis Distance: considering the curves as multivariate observations, the robust Mahalanobis distance between each curve and the pointwise sample mean is computed. Outliers are defined as observations that have squared robust Mahalanobis distances greater than the 0.99 quantile of a χ^2 distribution with p degrees of freedom, where p is the fixed number of observation points in every curve (see Hyndman and Shang (2010) and the references therein for details).
4. Integrated Squared Error (Hyndman and Ullah 2007): the integrated squared error between each curve in the sample and its projection into a given number K of robust principal components is computed. Outliers are defined as those observations with an integrated squared error greater than a threshold. Throughout this simulation

study K is chosen to be equal to 2 and the threshold is set to $s + 3.29\sqrt{s}$, where s is the median of the observed ISEs, as suggested in Hyndman and Shang (2010).

- 5, 6. Depth based weighting and trimming (Febrero et al. 2008): considering different depth measures for functional data the authors proposed to define as outliers the curves whose depth levels are below a cutoff. The cutoff is determined by a bootstrap procedure based either on trimming or weighting of the sample. In the first case, the proportion of potential outliers, which is used as trimming level, needs to be prespecified.
7. Projection based trimming (Fraiman and Svarc 2013): the authors propose a multivariate and functional robust estimation procedure that provides an outlier detection method as a by-product. The method consists on trimming the sample based on random projections. The maximum proportion of observations to be trimmed has to be prespecified.

For the sake of clarity and conciseness we restrict our simulation study to these seven methods. Comparison between these and some other related nonparametric procedures can be found in Hyndman and Shang (2010).

We have generated curves from three different models which are described next. In each case, $n - \lceil c \cdot n \rceil$ curves were generated according to the main model and the remaining $\lceil c \cdot n \rceil$ curves according to the contamination model, where for a real number x , $\lceil x \rceil$ is the smallest integer not less than x .

- Model 1. Main model: $X(t) = 30t(1 - t)^{3/2} + \varepsilon(t)$, and contamination model: $X(t) = 30t^{3/2}(1 - t) + \varepsilon(t)$, where $t \in [0, 1]$ and $\varepsilon(t)$ is a Gaussian process with zero mean and covariance function $\gamma(s, t) = 0.3 \exp\{-|s - t|/0.3\}$. This model had been already used in Febrero et al. (2008) and Fraiman and Svarc (2013).

- Model 2. Main model: $X(t) = 4t + \varepsilon(t)$, and contamination model: $X(t) = 4t + (-1)^u 1.8 + \frac{1}{\sqrt{2\pi 0.01}} \exp\{-(t - \mu)^2/0.02\} + \varepsilon(t)$, where $t \in [0, 1]$, $\varepsilon(t)$ is a Gaussian process with zero mean and covariance function $\gamma(s, t) = \exp\{-|s - t|\}$, u follows a Bernoulli distribution with probability 1/2 and μ is uniformly distributed in $[0.25, 0.75]$. The main model had been already used in Sun and Genton (2011).
- Model 3. Main model: $X(t) = 4t + \varepsilon(t)$, and contamination model: $X(t) = 4t + 2 \sin(4(t + \theta)\pi) + \varepsilon(t)$, where $t \in [0, 1]$, $\varepsilon(t)$ is a Gaussian process with zero mean and covariance function $\gamma(s, t) = \exp\{-|s - t|\}$ and θ is uniformly distributed in $[0.25, 0.75]$

For each one of the three models, we considered two different values for the sample size, $n = 50$ and 100 , and four values for the contamination rate, $c = 0.05, 0.1, 0.15$ and 0.2 , and we ran 200 simulations for each combination of n and c . In every case we sample the curves on 50 equidistant points over the interval $[0, 1]$. For the procedures requiring the specification of the coverage probability of the outlying region or trimming proportion we set those equal to the true value c . For procedures 5 and 6 we set to 200 the number of bootstrap samples and chose as depth function the modal depth (Cuevas et al. 2006) as advised in Febrero et al. (2008). For procedure 7 we set to 100 the maximum number of random projections. In Figure 4 we present the curves generated with each of these models in a single simulation run. In Tables 1 and 2 we show the results for the outliergram and the other seven methods in terms of the proportion of correctly identified outliers p_c (number of correctly identified outliers over the number of outliers in the sample) and the proportion of false positives p_f (number of wrongly identified outliers over the number of non-outlying curves in the sample). For Model 1, the method that achieves the best performance is the Robust Mahalanobis Distance whose p_c and p_f remain very high and low respectively across different sample sizes and contamination rates. However, this method's sensitivity for Models 2 and 3 is very low. On the contrary, the ISE method

performs very well on Models 2 and 3 and presents slightly worse results for Model 1. Let us point out that, although the sensitivity of this method is in general very high, its false detection rate is often larger than that of most of the methods. The functional boxplot has very low sensitivity in all the models as expected, since it is a method designed to detect magnitude outliers. The HDR functional boxplot detects more outliers than the functional boxplot, especially for $n = 100$, but as ISE, it exhibits very large false detection rates. With respect to the depth based methods (5 and 6), the trimming procedure works always better than the weighting procedure (except for $c = 0.05$ where their performances are similar) and they present better results for $n = 100$ than for $n = 50$. Except for Model 1 they seem to be quite resistant since their sensitivity remains almost constant as the contamination rate increases. That is also the case for the projection based procedure, whose sensitivity is, however, generally low and its false detection rate quite large across all models, sample sizes and contamination rates. With respect to the outliergram we can see that it presents very high p_c and low p_f in the three models, especially for $c = 0.05$ and $c = 0.1$. For Models 2 and 3 the sensitivity remains high for larger contamination rates, but it is true that for Model 1 it decreases rapidly as the contamination rate increases. Indeed, the outliergram is not a resistant procedure, since the presence of too many outlying trajectories would make decrease the MBD of all the curves in the sample making the (MEI,MBD) representation too spread to find outliers.

The simulations have been conducted in R using the functions implemented in the packages `fda.usc` (Febrero-Bande and Oviedo de la Fuente (2012), methods 5 and 6) and `rainbow` (Shang and Hyndman (2012), methods 2, 3 and 4). The R-code for the functional boxplot (Sun and Genton 2011) is provided as supplementary material of that paper and we have obtained the code for the projection based trimming method (Fraiman and Svarc 2013) from the authors. The R-code for our shape outlier detection method can be found in the supplementary materials. Its implementation relies on a fast

$n = 50, c = 0.05$		Model 1		Model 2		Model 3	
Method	p_c	p_f	p_c	p_f	p_c	p_f	
1. Fun. BP	0.48 (0.30)	0 (0.002)	0.14 (0.22)	0.004 (0.01)	0.17 (0.24)	0.005 (0.01)	
2. Fun. HDR BP	0.50 (0.19)	0.01 (0.01)	0.25 (0.22)	0.03 (0.01)	0.14 (0.19)	0.03 (0.01)	
3. Rob. Mah. Dist.	0.97 (0.12)	0.01 (0.02)	0.21 (0.24)	0.01 (0.02)	0.08 (0.19)	0.02 (0.03)	
4. ISE	0.73 (0.39)	0.04 (0.03)	1 (0.02)	0.08 (0.04)	1 (0)	0.08 (0.04)	
5. DB trimming	0.84 (0.245)	0 (0)	0.39 (0.23)	0.006 (0.01)	0.44 (0.28)	0.006 (0.01)	
6. DB weighting	0.98 (0.10)	0.005 (0.01)	0.51 (0.33)	0.008 (0.012)	0.51 (0.37)	0.006 (0.01)	
7. PB trimming	0.35 (0.23)	0.02 (0.01)	0.19 (0.19)	0.03 (0.01)	0.11 (0.17)	0.04 (0.01)	
8. Outliergram	1 (0.03)	0.02 (0.02)	0.97 (0.10)	0.04 (0.03)	1 (0.02)	0.05 (0.03)	
$n = 50, c = 0.1$		Model 1		Model 2		Model 3	
Method	p_c	p_f	p_c	p_f	p_c	p_f	
1. Fun. BP	0.42 (0.30)	0.001 (0.006)	0.11 (0.15)	0.003 (0.009)	0.15 (0.18)	0.005 (0.01)	
2. Fun. HDR BP	0.41 (0.16)	0.02 (0.02)	0.32 (0.17)	0.03 (0.02)	0.16 (0.16)	0.05 (0.02)	
3. Rob. Mah. Dist	0.95 (0.15)	0.007 (0.01)	0.21 (0.19)	0.01 (0.02)	0.07 (0.12)	0.02 (0.02)	
4. ISE	0.65 (0.39)	0.04 (0.03)	1 (0.02)	0.07 (0.04)	1 (0)	0.07 (0.04)	
5. DB trimming	0.65 (0.40)	0.001 (0.004)	0.44 (0.19)	0.007 (0.01)	0.44 (0.25)	0.009 (0.014)	
6. DB weighting	0.29 (0.38)	0.001 (0.004)	0.32 (0.25)	0.006 (0.01)	0.24 (0.25)	0.005 (0.01)	
7. PB trimming	0.37 (0.15)	0.03 (0.02)	0.23 (0.15)	0.04 (0.02)	0.13 (0.13)	0.05 (0.01)	
8. Outliergram	0.96 (0.11)	0.02 (0.02)	0.94 (0.13)	0.03 (0.03)	0.99 (0.05)	0.03 (0.02)	
$n = 50, c = 0.15$		Model 1		Model 2		Model 3	
Method	p_c	p_f	p_c	p_f	p_c	p_f	
1. Fun. BP	0.34 (0.24)	0 (0.003)	0.10 (0.13)	0.004 (0.01)	0.11 (0.15)	0.003 (0.009)	
2. Fun. HDR BP	0.35 (0.12)	0.03 (0.02)	0.33 (0.13)	0.03 (0.02)	0.20 (0.13)	0.06 (0.02)	
3. Rob. Mah. Dist	0.93 (0.16)	0.002 (0.007)	0.19 (0.19)	0.008 (0.02)	0.09 (0.15)	0.01 (0.02)	
4. ISE	0.61 (0.38)	0.04 (0.03)	0.99 (0.05)	0.07 (0.04)	1 (0.03)	0.07 (0.04)	
5. DB trimming	0.36 (0.41)	0.001 (0.006)	0.49 (0.20)	0.01 (0.02)	0.54 (0.30)	0.01 (0.02)	
6. DB weighting	0.009 (0.03)	0 (0)	0.14 (0.15)	0.003 (0.009)	0.09 (0.12)	0.003 (0.008)	
7. PB trimming	0.33 (0.11)	0.03 (0.02)	0.24 (0.13)	0.05 (0.02)	0.14 (0.10)	0.07 (0.02)	
8. Outliergram	0.64 (0.23)	0.004 (0.01)	0.83 (0.19)	0.01 (0.02)	0.95 (0.12)	0.01 (0.02)	
$n = 50, c = 0.2$		Model 1		Model 2		Model 3	
Method	p_c	p_f	p_c	p_f	p_c	p_f	
1. Fun. BP	0.27 (0.25)	0.004 (0.03)	0.08 (0.11)	0.002 (0.007)	0.07 (0.10)	0.001 (0.005)	
2. Fun. HDR BP	0.33 (0.10)	0.04 (0.02)	0.35 (0.11)	0.04 (0.03)	0.24 (0.12)	0.06 (0.03)	
3. Rob. Mah. Dist	0.88 (0.21)	0.004 (0.003)	0.16 (0.16)	0.005 (0.01)	0.09 (0.14)	0.01 (0.02)	
4. ISE	0.50 (0.35)	0.04 (0.03)	0.99 (0.04)	0.07 (0.04)	0.99 (0.03)	0.07 (0.04)	
5. DB trimming	0.25 (0.35)	0.001 (0.006)	0.50 (0.22)	0.01 (0.02)	0.54 (0.32)	0.02 (0.02)	
6. DB weighting	0.003 (0.02)	0(0)	0.08 (0.10)	0.002 (0.007)	0.04 (0.07)	0.002 (0.006)	
7. PB trimming	0.32 (0.11)	0.04 (0.03)	0.28 (0.10)	0.06 (0.03)	0.18 (0.09)	0.08 (0.02)	
8. Outliergram	0.35 (0.24)	0.001 (0.005)	0.64 (0.28)	0.006 (0.01)	0.81 (0.26)	0.005 (0.01)	

Table 1: The mean and the standard deviation (in parentheses) of the proportion of correctly and falsely identified outliers in the three simulation models for $n = 50$ and $c = 0.05, 0.1, 0.15$ and 0.2 .

$n = 100, c = 0.05$		Model 1		Model 2		Model 3	
Method	p_c	p_f	p_c	p_f	p_c	p_f	
1. Fun. BP	0.17 (0.21)	0 (0)	0.04 (0.09)	0 (0.002)	0.06 (0.11)	0 (0.003)	
2. Fun. HDR BP	0.67 (0.21)	0.02 (0.01)	0.32 (0.19)	0.04 (0.01)	0.13 (0.15)	0.05 (0.008)	
3. Rob. Mah. Dist.	0.99 (0.06)	0.009 (0.01)	0.20 (0.19)	0.01 (0.02)	0.05 (0.10)	0.01 (0.01)	
4. ISE	0.60 (0.40)	0.04 (0.02)	1 (0)	0.07 (0.03)	1 (0)	0.07 (0.03)	
5. DB trimming	1 (0.03)	0.002 (0.005)	0.75 (0.19)	0.02 (0.01)	0.85 (0.17)	0.02 (0.01)	
6. DB weighting	1 (0.05)	0.005 (0.007)	0.52 (0.26)	0.007 (0.009)	0.51 (0.29)	0.008 (0.009)	
7. PB trimming	0.51 (0.19)	0.03 (0.01)	0.29 (0.19)	0.04 (0.01)	0.14 (0.14)	0.05 (0.007)	
8. Outliergram	1 (0.01)	0.02 (0.02)	0.97 (0.07)	0.04 (0.02)	1 (0.01)	0.04 (0.02)	
$n = 100, c = 0.1$		Model 1		Model 2		Model 3	
Method	p_c	p_f	p_c	p_f	p_c	p_f	
1. Fun. BP	0.13 (0.15)	0 (0)	0.03 (0.06)	0 (0.002)	0.03 (0.06)	0 (0.002)	
2. Fun. HDR BP	0.64 (0.14)	0.04 (0.02)	0.44 (0.13)	0.06 (0.01)	0.22 (0.13)	0.09 (0.01)	
3. Rob. Mah. Dist	0.98 (0.07)	0.005 (0.008)	0.18 (0.13)	0.008 (0.01)	0.05 (0.09)	0.01 (0.01)	
4. ISE	0.62 (0.38)	0.035 (0.02)	1 (0.01)	0.07 (0.03)	1 (0)	0.06 (0.03)	
5. DB trimming	0.97 (0.16)	0.003 (0.006)	0.82 (0.13)	0.03 (0.01)	0.91 (0.13)	0.02 (0.01)	
6. DB weighting	0.39 (0.41)	0 (0.002)	0.30 (0.17)	0.004 (0.007)	0.21 (0.18)	0.004 (0.007)	
7. PB trimming	0.58 (0.15)	0.05 (0.02)	0.39 (0.13)	0.07 (0.01)	0.23 (0.12)	0.09 (0.01)	
8. Outliergram	0.97 (0.07)	0.01 (0.01)	0.95 (0.09)	0.02 (0.02)	1 (0.02)	0.02 (0.01)	
$n = 100, c = 0.15$		Model 1		Model 2		Model 3	
Method	p_c	p_f	p_c	p_f	p_c	p_f	
1. Fun. BP	0.07 (0.11)	0 (0)	0.03 (0.05)	0 (0.001)	0.03 (0.05)	0 (0.002)	
2. Fun. HDR BP	0.63 (0.13)	0.07 (0.02)	0.50 (0.11)	0.01 (0.02)	0.30 (0.13)	0.12 (0.02)	
3. Rob. Mah. Dist	0.97 (0.07)	0.001 (0.004)	0.15 (0.13)	0.005 (0.008)	0.05 (0.08)	0.01 (0.01)	
4. ISE	0.52 (0.36)	0.03 (0.02)	1 (0.02)	0.07 (0.03)	1 (0)	0.06 (0.03)	
5. DB trimming	0.85 (0.33)	0.003 (0.006)	0.87 (0.11)	0.04 (0.02)	0.95 (0.10)	0.04 (0.02)	
6. DB weighting	0.004 (0.02)	0 (0.001)	0.15 (0.13)	0.003 (0.005)	0.07 (0.09)	0.003 (0.006)	
7. PB trimming	0.61 (0.11)	0.07 (0.02)	0.45 (0.11)	0.10 (0.02)	0.28 (0.10)	0.13 (0.02)	
8. Outliergram	0.67 (0.20)	0.006 (0.009)	0.87 (0.12)	0.01 (0.01)	0.98 (0.04)	0.01 (0.01)	
$n = 100, c = 0.2$		Model 1		Model 2		Model 3	
Method	p_c	p_f	p_c	p_f	p_c	p_f	
1. Fun. BP	0.06 (0.08)	0 (0)	0.02 (0.03)	0 (0)	0.02 (0.03)	0 (0)	
2. Fun. HDR BP	0.60 (0.10)	0.10 (0.0)	0.56 (0.10)	0.11 (0.02)	0.41 (0.13)	0.15 (0.03)	
3. Rob. Mah. Dist.	0.92 (0.11)	0 (0.001)	0.13 (0.10)	0.003 (0.006)	0.07 (0.11)	0.008 (0.01)	
4. ISE	0.44 (0.33)	0.03 (0.02)	0.99 (0.03)	0.06 (0.03)	1 (0.01)	0.05 (0.03)	
5. DB trimming	0.48 (0.46)	0.002 (0.005)	0.88 (0.11)	0.04 (0.02)	0.94 (0.11)	0.03 (0.02)	
6. DB weighting	0.002 (0.01)	0 (0)	0.08 (0.08)	0.001 (0.004)	0.04 (0.05)	0.002 (0.005)	
7. PB trimming	0.63 (0.10)	0.09 (0.02)	0.50 (0.10)	0.12 (0.02)	0.34 (0.09)	0.16 (0.02)	
8. Outliergram	0.19 (0.14)	0.001 (0.005)	0.66 (0.21)	0.003 (0.006)	0.85 (0.18)	0.002 (0.005)	

Table 2: The mean and the standard deviation (in parentheses) of the proportion of correctly and falsely identified outliers in the three simulation models for $n = 100$ and $c = 0.05, 0.1, 0.15$ and 0.2 .

Method	<i>Time(sec.)</i>
1. Functional Boxplot	3.789
2. Functional HDR Boxplot	1.911
3. Robust Mahalanobis Distance	0.718
4. Integrated Squared Error	0.210
5. Depth based trimming	83.969
6. Depth based weighting	84.903
7. Projection based trimming	0.013
8. Outliergram	0.380

Table 3: Computing time (in seconds) for the different methods on a sample of 100 curves generated under Model 1 with 50 observation points by curve and contamination rate equal to 0.1.

computation of the modified band depth and modified epigraph index as done in the R package `Depth.Tools` (López-Pintado and Torrente (2013); see also Sun et al. (2012)). In Table 3 we show the computing time required by each of the methods to run on a sample of 100 curves in the implementations mentioned before and with the configurations used through the simulation study (R 3.0.0 on a Mac OS X 10.8.3, 2.9 GHz, 8GB of RAM). For the functions that produce graphics, the running time with the graphic option disabled is considered.

5 Application

In order to further asses the performance of the outliergram in the detection of shape outliers we now apply it to real data. The well known Berkeley growth data set contains height curves from 54 girls and 39 boys measured at 31 fixed time points between 0 and 18 year old (see Ramsay and Silverman (2005) for details). This dataset is publicly available in R in the `fda` package (Ramsay et al. 2013) among others. A preliminary analysis performed in each group separately is summarized in Table 4, where we present the number of detected outliers in each group by the different methods described in the previous section. For the methods requiring the specification of an expected outlier rate the value 0.05 has been considered. In Figure 5 we present the original curves and

the corresponding outliergrams. In the girls sample, curve 8, a magnitude outlier, is identified by all the methods whereas in the boys sample there is no such consensus. The next step in our analysis is to contaminate the girls sample with boys curves and viceversa. Although boys are in general taller than girls such contamination is not purely of magnitude nature. Indeed, the shapes of typical height curves in both groups are different in the sense that the pubertal spurt appears at different ages in boys and girls and with a different velocity rate. We have introduced 6 randomly chosen boys curves in the girls sample and 4 randomly chose girls curves in the boys sample so that the contamination rate was in both cases around 0.1. However, in the girls sample we have also considered as an outlier observation number 8, so for the methods requiring the specification of an expected proportion of outliers the rates $7/60$ and $4/39$ have been considered for the girls and boys samples respectively. We have randomly repeated this procedure 200 times and the average and standard deviations of the rates of correctly and wrongly identified outliers by the different are presented in Table 5. For the girls sample, the best results in terms of correctly identified outliers are achieved by the Integrated Squared Error rule and the outliergram with a percentage of 73%, although the former has a false positive rate of 25% whereas the latter's is only 4% in average. With respect to the boys sample, the percentage of correctly identified outliers is significantly larger for the ISE method than for the functional HDR boxplot or the outliergram with a value of 93% versus 49% and 41%, respectively. However, the false positive rate of ISE is again too large, whereas the ones for the functional HDR boxplot or the outliergram are similar and acceptable (5% and 2% respectively). Thus, the functional HDR boxplot and the outliergram have similar performances in this example although it is important to recall that the former has been given the true number of outliers in the sample whereas the latter runs without any *a priori* information. With respect to the outliergram let us point out that in the girls sample curves 3, 8 and 32 are consistently identified as outliers

Method	Girls sample	Boys sample
1. Functional Boxplot	8	-
2. Functional HDR Boxplot	8, 25, 48	29, 37
3. Robust Mahalanobis Distance	8, 13	37
4. Integrated Squared Error	1, 3, 6, 8, 10, 15, 17, 18, 25, 26, 29, 32, 37, 38, 42, 49, 53	1, 12, 15, 18, 23, 24, 26, 34, 35, 36, 37, 38
5. Depth based trimming	8	-
6. Depth based weighting	8	-
7. Projection based trimming	8, 13, 25	1, 29
8. Outliergram	3, 8, 32	9, 28, 36

Table 4: Outliers detected by the different methods in the girls and boys height curves samples.

Method	Girls contaminated sample		Boys contaminated sample	
	p_c	p_f	p_c	p_f
1. Functional Boxplot	0.15 (0.02)	0 (0)	0.05 (0.12)	0 (0)
2. Functional HDR Boxplot	0.53 (0.14)	0.04 (0.02)	0.49 (0.31)	0.05 (0.03)
3. Robust Mahalanobis Distance	0.22 (0.18)	0 (0)	0.21 (0.26)	0.01 (0.02)
4. Integrated Squared Error	0.73 (0.15)	0.25 (0.04)	0.93 (0.15)	0.31 (0.04)
5. Depth based trimming	0.29 (0.13)	0 (0)	0.26 (0.24)	0.006 (0.03)
6. Depth based weighting	0.19 (0.07)	0 (0)	0.13 (0.16)	0 (0)
7. Projection based trimming	0.36 (0.14)	0.07 (0.018)	0.18 (0.18)	0.08 (0.02)
8. Outliergram	0.73 (0.15)	0.04 (0.003)	0.41 (0.22)	0.02 (0.02)

Table 5: The mean and the standard deviation (in parentheses) of the proportion of correctly and falsely identified outliers in the growth curves application. The first two columns show the results for the girls data set contaminated 200 times with 6 boy height curves chosen at random. The second two columns show the results for the boys data set contaminated 200 times with 4 girl height curves chosen at random.

across different contaminations of the sample with boys curves as well as in the original sample. However, for the boys sample, curves 9, 28 and 36 were identified as outliers in the original sample but not in many of the contaminated samples (see Figure 5 for an example). Indeed, looking at the outliergrams of the original girls and boys samples one can see that in the second case the separation between outlying and non-outlying observation is not as clear as in the first one. So, even if the rule classified boys curves 9, 28 and 36 as outliers, in this case the visualization of the outliergram may be useful to discard this possibility.

6 Discussion

This article propose the outliergram as a tool for representing functional observations in the plane in terms of shape. It allows to visually asses sample variability in terms of shape and to detect potential shape outliers. Indeed, the more similar and smooth the curves in the sample, the closer to the parabola (1) the points in the outliergram. On the other hand, the more noisy the curves and the larger number of crossing points between them, the more dispersed the points under (1) in the outliergram. In both cases, the points with the largest distances to the parabola represent the most outlying curves, in terms of shape, of the sample.

In addition to the visualization tool we propose a boxplot-based rule on the distances to the parabola (1) to classify observation into outlying and non-outlying in terms of shape. We suggest to combine it with the functional boxplot (Sun and Genton 2011) to also account for magnitude outliers. Although we have shown its accuracy at detecting outliers on simulated and real data we suggest to always visualize the outliergram for deeper understanding of the nature of the sample and the classifying rule.

Supplemental materials

R-code: R-function for the shape outlier detection algorithm and visualization tool described in this paper (OutGram.R). We also include four other R files with an example of use (example.R), the code for replication of the simulation study conducted in Section 4 (simus.R), the code for replication of the analysis of growth data conducted in Section 5 (growth_app.R) and the code to evaluate the computing time of the different methods (runningtime.R). All files can be found in a single zip file (R_CODE_OutlierGram.zip).

Acknowledgments

The authors acknowledge financial support from grant ECO2011-25706, Spain. The first author also acknowledge financial support from grant MTM2010-17323, Spain. We are grateful to Marcela Svarc who provided us with the R code for the implementation of the method described in Fraiman and Svarc (2013).

Appendix

Proof of Remark 1. Let $B_{i,j,x} = \{t \in \mathcal{I}, \min(x_i(t), x_j(t)) \leq x(t) \leq \max(x_i(t), x_j(t))\}$.

Then we can write

$$MBD_{\{x_1, \dots, x_n\}}(x) = \binom{n}{2}^{-1} \sum_{i=1}^n \sum_{j=i+1}^n \frac{\lambda(B_{i,j,x})}{\lambda(\mathcal{I})} = \frac{2}{n(n-1)\lambda(\mathcal{I})} \sum_{i=1}^n \sum_{j=i+1}^n \lambda(B_{i,j,x}).$$

It is easy to see that $B_{i,j,x} = (E_{i,x} \cap \overline{E}_{j,x}) \cup (\overline{E}_{i,x} \cap E_{j,x})$ if $x \neq x_i, x \neq x_j$ and $B_{i,j,x} = \mathcal{I}$ otherwise, where \overline{A} denotes the complement of set A . Then

$$\lambda(B_{i,j,x}) = \begin{cases} \lambda(E_{i,x}) + \lambda(E_{j,x}) - 2\lambda(E_{i,x} \cap E_{j,x}) & \text{if } x \neq x_i, x \neq x_j \\ 2\lambda(E_{i,x}) + \lambda(E_{j,x}) - 2\lambda(E_{i,x} \cap E_{j,x}) & \text{if } x = x_i \\ \lambda(E_{i,x}) + 2\lambda(E_{j,x}) - 2\lambda(E_{i,x} \cap E_{j,x}) & \text{if } x = x_j \end{cases}$$

so we get

$$\begin{aligned}
\sum_{i=1}^n \sum_{j=i+1}^n \lambda(B_{i,j,x}) &= \sum_{i=1}^n \sum_{j=i+1}^n [\lambda(E_{i,x}) + \lambda(E_{j,x}) - 2\lambda(E_{i,x} \cap E_{j,x})] + \sum_{i=1}^n \lambda(E_{i,x}) - \lambda(\mathcal{I}) \\
&= (n-1) \sum_{i=1}^n \lambda(E_{i,x}) - 2 \sum_{i=1}^n \sum_{j=i+1}^n \lambda(E_{i,x} \cap E_{j,x}) + \sum_{i=1}^n \lambda(E_{i,x}) - \lambda(\mathcal{I}) \\
&= (n+1) \sum_{i=1}^n \lambda(E_{i,x}) - 2 \sum_{i=1}^n \sum_{j=i+1}^n \lambda(E_{i,x} \cap E_{j,x}) - \sum_{i=1}^n \lambda(E_{i,x}) - \lambda(\mathcal{I}) \\
&= n(n+1) \frac{1}{n} \sum_{i=1}^n \lambda(E_{i,x}) - \sum_{i=1}^n \sum_{j=1}^n \lambda(E_{i,x} \cap E_{j,x}) - \lambda(\mathcal{I}).
\end{aligned}$$

Then,

$$\begin{aligned}
MBD_{\{x_1, \dots, x_n\}}(x) &= \frac{2}{n(n-1)\lambda(\mathcal{I})} \sum_{i=1}^n \sum_{j=i+1}^n \lambda(B_{i,j,x}) \\
&= \frac{-2}{n(n-1)} + \frac{2(n+1)}{(n-1)} MEI_{\{x_1, \dots, x_n\}}(x) - \frac{2}{n(n-1)} \left[\sum_{i=1}^n \sum_{j=1}^n \frac{\lambda(E_{i,x} \cap E_{j,x})}{\lambda(\mathcal{I})} \right].
\end{aligned}$$

□

References

- A. Cuevas, M. Febrero, and R. Fraiman. On the use of bootstrap for estimating functions with functional data. *Computational Statistics and Data Analysis*, 51:1063–1074, 2006.
- M. Febrero, P. Galeano, and W. González-Manteiga. Outlier detection in functional data by depth measures, with application to identify abnormal NOx levels. *Environmetrics*, 19:331–347, 2008.
- M. Febrero-Bande and M. Oviedo de la Fuente. Statistical computing in functional data analysis: The R package fda.usc. *Journal of Statistical Software*, 51(4):1–28, 2012. URL <http://www.jstatsoft.org/v51/i04/>.
- R. Fraiman and M. Svarc. Resistant estimates for high dimensional and functional data

- based on random projections. *Computational Statistics & Data Analysis*, 58:326–338, 2013.
- D. Gervini. Detecting and handling outlying trajectories in irregularly sampled functional datasets. *The Annals of Applied Statistics*, 3:1758–1775, 2009.
- D. Gervini. Outlier detection and trimmed estimation for general functional data. *Statistica Sinica*, 22:1639–1660, 2012.
- R. J. Hyndman. Computing and graphing highest density regions. *The American Statistician*, 50:120–126, 1996.
- R. J. Hyndman and H.L. Shang. Rainbow plots, bagplots, and boxplots for functional data. *Journal of Computational and Graphical Statistics*, 19:29–49, 2010.
- R. J. Hyndman and M. S. Ullah. Robust forecasting of mortality and fertility rates: A functional data approach. *Computational Statistics & Data Analysis*, 52:4924–4956, 2007.
- S. López-Pintado and J. Romo. On the concept of depth for functional data. *Journal of the American Statistical Association*, 104(486):718–734, 2009.
- S. López-Pintado and J. Romo. A half-region depth for functional data. *Computational Statistics & Data Analysis*, 55:1679–1695, 2011.
- S. López-Pintado and A. Torrente. *depthTools: Depth Tools Package*, 2013. URL <http://CRAN.R-project.org/package=depthTools>. R package version 0.3.
- B. Martín-Barragán, R. Lillo, and J. Romo. Functional boxplots based on half-regions. Universidad Carlos III de Madrid, Working paper series, 2012.
- J. O. Ramsay, H. Wickham, S. Graves, and G. Hooker. *fda: Functional Data Analysis*, 2013. URL <http://CRAN.R-project.org/package=fda>. R package version 2.3.4.

- J.O. Ramsay and B.W. Silverman. *Functional Data Analysis*. Springer Series in Statistics, 2005.
- H.L. Shang and R. J. Hyndman. *rainbow: Rainbow plots, bagplots and boxplots for functional data*, 2012. URL <http://CRAN.R-project.org/package=rainbow>. R package version 3.1.
- Y. Sun and M. G. Genton. Functional boxplots. *Journal of Computational and Graphical Statistics*, 20:316–334, 2011.
- Y. Sun, M. G. Genton, and D. C. Nychka. Exact fast computation of band depth for large functional datasets: How quickly can one million curves be ranked? *Stat*, 1: 68–74, 2012.

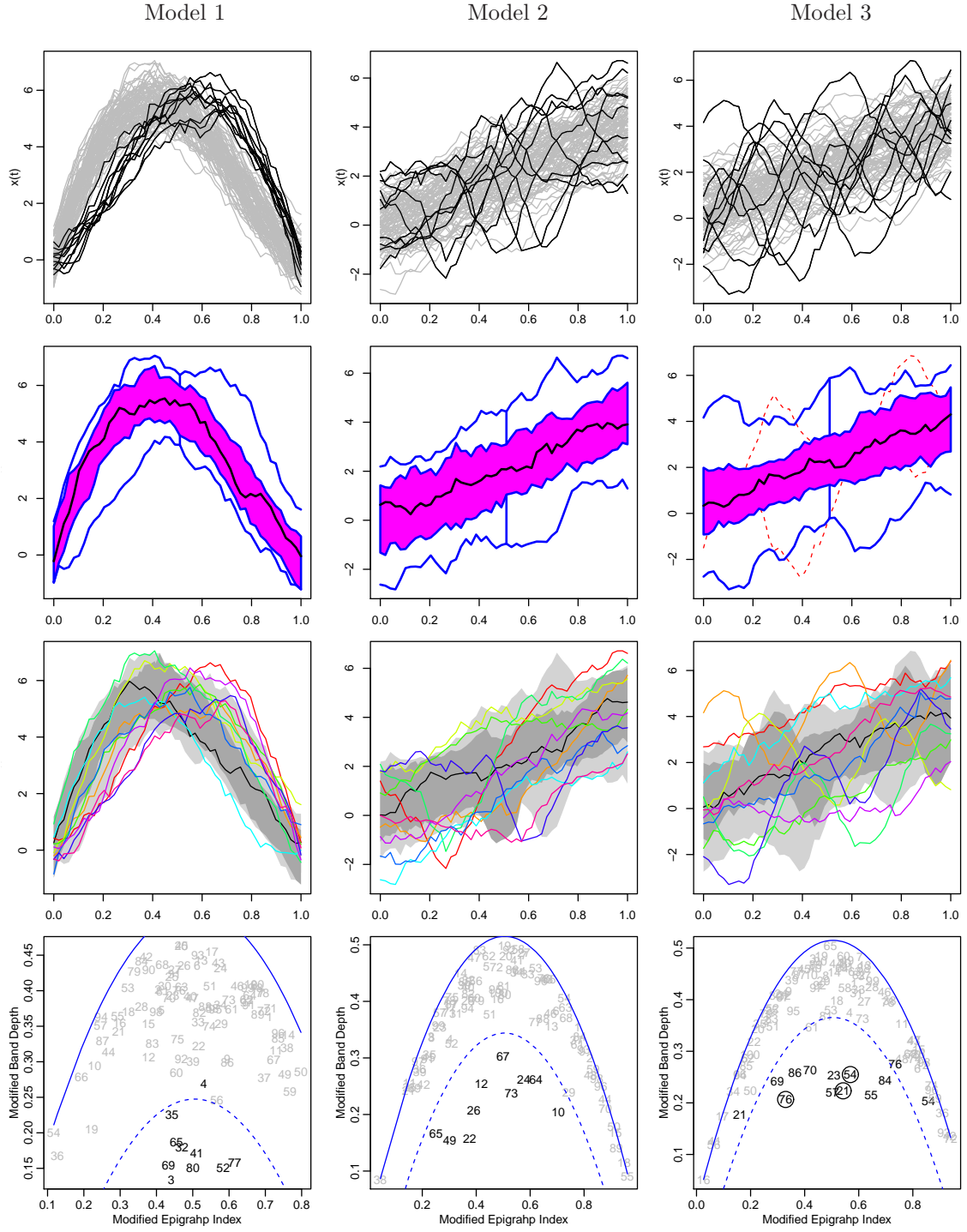


Figure 4: Three simulation runs from models 1, 2, and 3 with $n = 100$ and $c = 0.1$. First row: curves generated from the main model (gray) and the contamination model (black). Second row: Functional Boxplot (outliers are red-dashed line). Third row: Functional HDR Boxplot (outliers are colored lines). Fourth row: Outliergram (outliers correspond to the points below the dashed parabola; the code color is the same of the first row; circles stand for curves that have been considered outlier after having been shifted vertically towards the center of the sample).

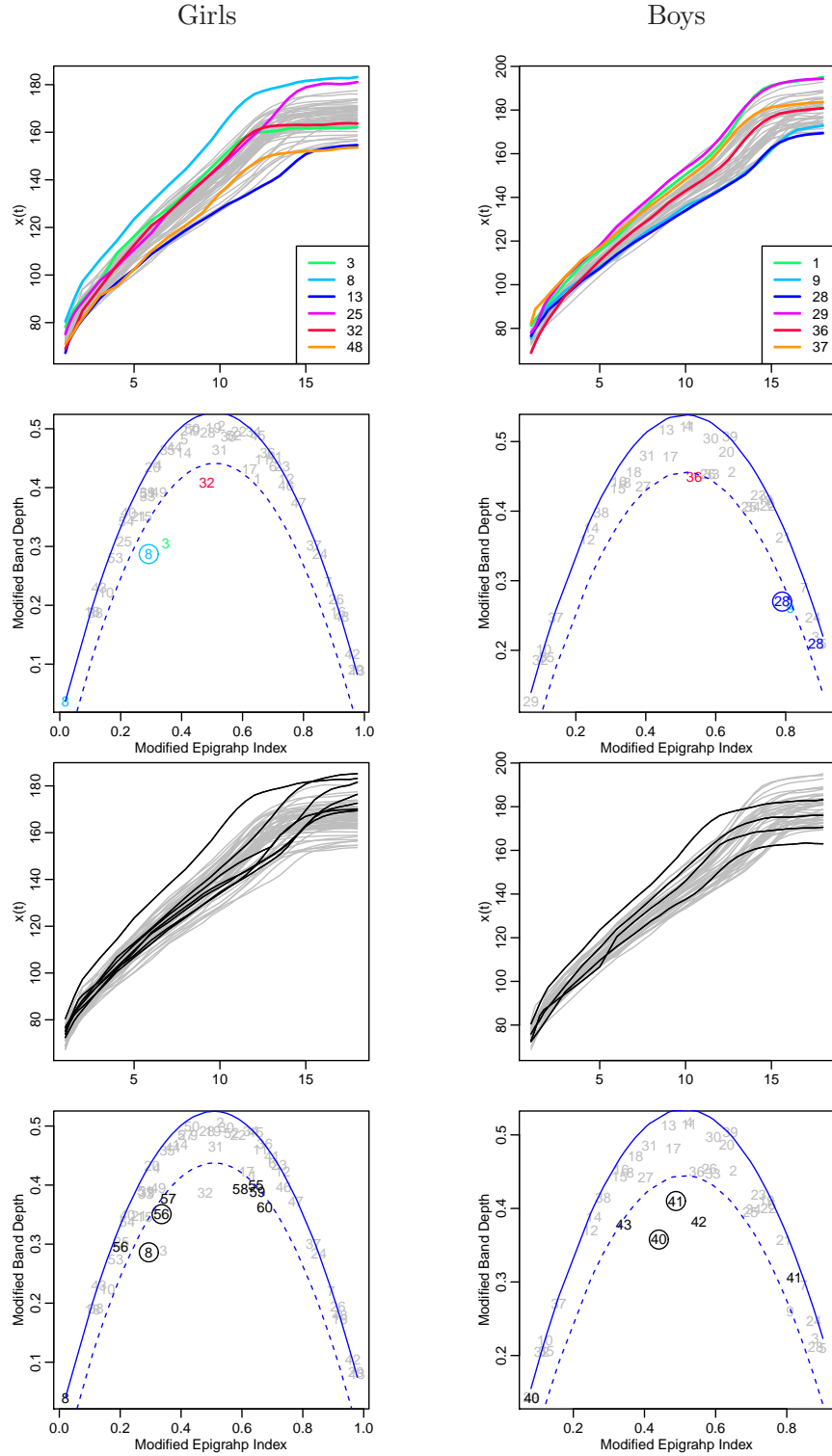


Figure 5: Observed curves and outliergrams for the girls and boys growth curves (first two rows). Some of the outliers found by the different methods are displayed in color (see Table 4). Third and Fourth rows: contaminated samples with the *true* outliers in black and the corresponding outliergrams.